ON THE INSTABILITY OF SOLITONS IN SHEAR HYDRODYNAMIC FLOWS

Sergey K. Zhdanov

Plasma Physics Department,

Moscow Engineering Physics Institute,

Kashirskoe sh. 31, Moscow, 115409, Russia

Denis G. Gaidashev

Physics Department,

University of Texas at Austin,

C1600, Austin, Texas, 78712

tel: (512) 453 1779,

e-mail: gaidash@math.utexas.edu

August 16, 2002

Abstract

The paper presents a stability analysis of plane solitons in hydrodynamic shear flows obeying a (2+1) analogue of the Benjamin-Ono equation. The analysis is carried out for the Fourier transformed linearized (2+1) Benjamin-Ono equation. The instability region and the short-wave instability threshold for plane solitons are found numerically. The numerical value of the perturbation wave number at this threshold turns out to be constant for various angles of propagation of the solitons with respect to the main shear flow. The maximum of the growth rate decreases with the increasing angle and becomes equal to zero for the perpendicular propagation. Finally, the dependency of the growth rate on the propagation angle in the long-wave limit is determined and the existence of a critical angle which separates two types of behavior of the growth rate is demonstrated.

Keywords:

Benjamin-Ono equation; Stability of solitons; Stratified flows; Self-focusing instability; Two-dimensional long-wave models.

1 INTRODUCTION

Stability of non-linear waves in various hydrodynamic models, in particular, stability of solitons, has been historically of much interest. Solitons were shown to be typical of many non-linear evolution equations, extensive theoretical and experimental study of these objects undertaken by the present time has revealed the unique features of these waves.

An interesting case of solitary waves existing in hydrodynamic flows is solitons propagating in a stationary shear flow. Stability of these waves is the focus of the present paper. It has been shown [1], [2] that the propagation of solitons in shear flows of ideal deep fluid in the one-dimensional case is described by the well-known Benjamin-Ono equation

$$u_t + 6uu_x + \partial_x^2 \hat{H}[u] = 0 \qquad (1.1)$$

here, u is the perturbation of the horizontal velocity of the main flow and

$$\hat{H}[u] = \frac{1}{\pi} \int\limits_{-\infty}^{+\infty} \frac{u(x')}{x - x'} dx' \quad (1.2)$$

is the Hilbert transform of u. The factor in front of the non-linear term can be chosen to be an arbitrary constant by a simple rescaling. The most often used factors are 2 and 6.

Periodic solutions of the Benjamin-Ono equation can be obtained by Hirota's direct method [4], [5] and appear as follows

$$u = \frac{1}{3} \frac{k_1 \cdot \tanh \phi_1}{1 + \frac{\cos \xi_1}{\cosh \phi_1}} \qquad (1.3)$$

$$\xi_1 = k_1(x - c_1 t) + \xi_1^{(0)}, \quad c_1 = k_1 \coth \phi_1$$

here $\xi_1^{(0)}$ is a constant phase shift; parameters k_1 and ϕ_1 are positive constants, the first being the wave number, the second - the non-linearity parameter. The case of the last parameter $\phi_1 \to \infty$ leads to a harmonic wave of the small amplitude, while the case of $\phi_1 \to 0$ and $k_1 \to 0$ keeping the ratio $\frac{k_1}{\phi_1}$ bounded gives a plane "algebraic" soliton (in this paper by "plane soliton" we shall mean the standard $1-D$ soliton, "carpet roll" extending to infinities in the direction perpendicular to the direction of propagation) of the form

$$u = \frac{2}{3}\frac{S}{1+(S\xi_1 - \Omega t)^2}, \quad S = \frac{k_1}{\phi_1}, \quad \Omega = S^2 \qquad (1.4)$$

Bi-soliton solutions and multi-soliton solutions could be obtained by Hirota's method (see [5]) introducing more parameters k_i, ϕ_i, c_i and variables ξ_i in a similar way.

The two-dimensional waves in a stratified hydrodynamic flow were first considered in [3]. Starting from the Euler equations with the standard "solid" surface and bottom conditions the author has obtained the well-known Rayleigh equation for the amplitude of the vertical velocity of linear plane waves $W(z)\exp[i(\mathbf{kx}-\omega t)]$ (here, z is the vertical coordinate, $\mathbf{x}=(x,y)$)

$$(U(z)-c)(W''(z)-k^2W(z)) - U''(z)W(z) = 0 \qquad (1.5)$$

where $U(z)$ is the main flow assumed to be dependent on z only. Solutions (modes) of (1.4) are known to be stable in the limit $k \to 0$ for the flow profiles without points of inflection. It has been shown in [3] that in long-wave approximation ($kh << 1$, h - the typical vertical scale of the flow) the linear analysis yields a localized mode

$$W(z) = (U-c)\exp[-k\,|z|]$$

with the dispersion

$$c = U(0) + k \left[\frac{U^2}{U'}\right]_{z=0} \qquad (1.6)$$

Further, as shown in [3], the standard technique of the expansion in a small parameter gives a non-linear integro-differential equation for the amplitude of a small perturbation of the horizontal velocity of the main flow, $A(\mathbf{x},t)$

$$A_t + \nu A_x + sAA_x - r\hat{G}[A_x] = 0 \qquad (1.7)$$

$$\hat{G}[A(\mathbf{x}, t)] = \int\int k' A(\mathbf{x}',t) \exp[i\mathbf{k}'(\mathbf{x}-\mathbf{x}')]\partial\mathbf{x}'\partial\mathbf{k}'$$

$$\nu = U(0), \qquad s = [U'(z)]_{z=0}\,, \qquad r = \left[\frac{U^2}{U'}\right]_{z=0}$$

here $\mathbf{x}=(x, y)$ and $\mathbf{k}=(k_x, k_y)$. We shall call (1.7) the Shrira equation after the author of [3]. It should be noted that this equation is a two-dimensional analogue of the Benjamin-Ono equation and coincides with the latter in reduction $A(x, y, t) = A(x, t)$.

The theoretical analysis of the transverse instability of the Benjamin-Ono solitons in the two-dimensional case is given in [6]. The authors show that such solitons should have self-focusing instability which results in a collapse at later stages. Such collapsing objects were simulated in [7]. The transverse instability was also studied in [8]: analytically for long-wave transverse perturbations of the amplitude and numerically in general case. It is worth noting that numerical analysis in [8] based upon the method suggested in [7] gives the untypical dependence of the instability growth rate on the perturbation wave number. For large inclination angles of solitons this dependence becomes oscillating, eventually, for angles close to $\frac{\pi}{2}$ there appear many regions of instability with the growth rate intermittently increasing to a positive maximum and dropping back to zero as the perturbation wave number increases.

2 (2+1) BENJAMIN-ONO EQUATION AS A MODEL EQUATION FOR SHEAR FLOWS

Before we proceed to the stability analysis of Benjamin-Ono solitons in one- and two-dimensional cases we want to briefly illustrate the derivation of (1.6) on a plasma-related system (unlike in the original paper [3]). We will present the general guidelines leaving the detailed calculations to the interested reader.

We consider a very popular magneto-hydrodynamic (MHD) system in plasma physics - a flow of electrons with a velocity profile sheared in one direction (by our convention - vertical direction). Linear perturbations of the vertical component of the velocity of a cold electron shear flow, $w = W(z)\exp[i(k_x x - \omega t)]$, are described by the following equation (see, for example [10])

$$\frac{\partial}{\partial z}\frac{1}{\varepsilon}\frac{\partial}{\partial z}(\hat{\omega}\varepsilon W) - k_x^2\hat{\omega}W = 0 \qquad (2.1)$$

$$\varepsilon = 1 - \frac{\omega_p^2}{\hat{\omega}^2}, \qquad \hat{\omega} = \omega - k_x U(z)$$

where ω, k_x are frequency and wave number of the transverse perturbations; ω_p is the electron plasma frequency; $U(z)$ is the unperturbed profile of the initial non-uniform flow along the x-axis, $\mathbf{U}(z) = U(z)\hat{\mathbf{x}}$. Low frequency perturbation ($\omega_p^2 >> (\omega - k_x U(z))^2$) gives us the standard Rayleigh equation (1.5).

In what follows we consider the main flow with two different flow profiles (Fig.1). The following standard (derivation can be found, for ex. in [10]) system of MHD equations holds for such flow

$$\mathbf{u}_{\mathrm{t}} + (\mathbf{U}{+}\mathbf{u})\nabla(\mathbf{U}{+}\mathbf{u}) = \frac{e}{m}\nabla\phi \qquad (2.2a)$$

$$n_t + n_0\nabla\mathbf{u}{+}\nabla(n(\mathbf{U}{+}\mathbf{u})) = 0 \qquad (2.2b)$$

$$\Delta\phi = 4\pi n \qquad (2.2c)$$

with the boundary condition at the "solid" edges of the electron flow (beam): $w(0) = 0$ and $w(-h) = 0$, with h being the width of the beam. In (2.2) $\mathbf{U}$ is the unperturbed flow velocity, and n_0 is the unperturbed plasma concentration treated as a constant value; $\mathbf{u}{=}(u, v, w)$, n and ϕ are perturbations of the velocity, electric potential and concentration ; e and m are the absolute value of electron charge and mass.

Applying the multiple scale expansion proposed in [9] and used in [3] to obtain equation (1.7) we introduce the following scaling of variables

$$u' = u, v' = v, w' = \frac{w}{\varepsilon}, \phi' = \phi, \xi = \varepsilon z, \mu = \varepsilon y, \theta = \varepsilon(x{-}Ut), \tau = \varepsilon^2 t \qquad (2.3)$$

where the small parameter, $\varepsilon = kh << 1$, should be considered as an expansion parameter. System (2.2) written up to the first order in ε is nothing but the linearized version of (2.2), the same system written in the second order of ε suggests the following ansatz for the velocity x-component

$$u = A(\theta, \mu, \xi, \tau)U'(z) \qquad (2.4)$$

We notice that this expression contains two disparate scales along z. Amplitude A obeys one of the two equations corresponding to the flow profiles pictured in Fig.1a and Fig.1b respectively.

$$A_\tau + U' A A_\theta - \frac{U^2}{U'} \hat{G}[A_\theta] = 0 \qquad (2.5a)$$

$$A_\tau + U' A A_\theta + \frac{U^2}{U'} \hat{G}[A_\theta] = 0 \qquad (2.5b)$$

where $\hat{G}$ is the integral operator

$$\hat{G}[A(\mathbf{x},t)] = \int\int k' \coth[k'h] A(\mathbf{x}',t) \exp[i\mathbf{k}'(\mathbf{x}-\mathbf{x}')] \partial\mathbf{x}' \partial\mathbf{k}'$$

In the limiting case of a very thick electron beam (very deep layer of fluid), $h \to \infty$, $\hat{G}$ coincides with the operator in equation (1.7). By a simple rescaling and nondimensionalization of the variables these two equations can be written in the standard Benjamin-Ono form

$$A_\tau + 6AA_\theta \pm \hat{G}[A_\theta] = 0 \qquad (2.6)$$

The above equation (for any choice of sign) describes waves propagating downstream slower then the main flow (upstream in the frame fixed on the main flow). Physically, solitons of these equations are depressions in the flow profile of the amplitude ("depth" of depressions) decreasing in the z-direction. The direction of propagation (in the frame of reference fixed on the main flow) coincides with the direction of the linear waves for the surface flow in Fig.1a (minus sign) and is opposite to the direction of the linear waves for the boundary flow in Fig.1b (plus sign).

The example of the electron flow considered above (although of somewhat sketchy character) demonstrates the possibility of extending the application of Shrira equation. Solitons of this equation have not been discussed in plasma applications, but taking into consideration the fact that non-uniform flows are typical for plasmas, one could expect that algebraic solitons might appear in such systems.

3 SOME REMARKS ABOUT THE STABILITY OF SOLITONS WITH RESPECT TO LONGITUDINAL PERTURBATIONS

In this section we want to briefly comment on the problem of stability of the solitons of the (1+1) Benjamin-Ono equation. We shall consider the Benjamin-Ono equation in the form

$$u_t + 6uu_x + \partial_x^2 \hat{H}[u] = 0 \qquad (3.1)$$

which has the following well-known "algebraic" soliton solution

$$u_0 = \frac{2}{3} \frac{S}{1 + (Sx - \Omega t)^2}, \qquad \Omega = S^2 \qquad (3.2)$$

where S is an arbitrary parameter defining velocity or amplitude of a soliton.

Let us consider the stability of the Benjamin-Ono solitons under the longitudinal perturbations. We proceed to linearize the Benjamin-Ono equation for

$$u = u_0 + \tilde{u}(x - St, t) \qquad (3.3)$$

here u_0 is the Benjamin-Ono soliton (3.2) and $\tilde{u}$ - perturbation of a small amplitude. Translational invariance necessitates that the gradient of the soliton solution be an eigenfunction of the linearized problem.

The equation for the Fourier transform $\tilde{\phi}(q, \omega)$ of the potential function $\phi(x, t)$ $(\phi(x, t)_x = u(x, t))$ in the linearized problem can be shown to be

$$(\partial_q^2 - \sigma^2)(-\omega\tilde{\phi} + \frac{q}{\sigma}\tilde{\phi} + q\,|q|\,\tilde{\phi}) + 4\sigma^2 q\tilde{\phi} = 0 \qquad (3.5)$$

where $\sigma = \frac{1}{S}$. Equivalently, this equation could be written for function χ satisfying $\tilde{\phi} = \chi_{qq} - \sigma^2 \chi$

$$\chi_{qq} - \left(\sigma^2 + \frac{4\sigma}{\frac{1}{\sigma} + |q| - \frac{\omega}{q}} \right) \chi = 0 \qquad (3.6)$$

Localized solution of this equation for perturbations with the stationary amplitude ($\omega = 0$) could be presented as

$$\chi(q) = const \cdot q(1 + \sigma\,|q|) \exp[-\sigma\,|q|] \qquad (3.7)$$

which, in accordance with our above remark about translational invariance, predictably gives a solution in the form of a soliton (3.2) after the inverse Fourier transformation. In a more general case of the time-dependent perturbations we found a particular solution of (3.6) directly; it can be presented in the form

$$\phi(x,t) = A(-i\chi(k) + \frac{1 + 2\chi(k)\sigma}{\theta - i\sigma}) \exp[-i(\omega t + kx)] \qquad (3.8)$$

where A is an arbitrary constant amplitude of the perturbation.

Stability of the Benjamin-Ono solitons with respect to longitudinal perturbations is a well-known fact. Perturbation (3.8) does not destroy a Benjamin-Ono soliton as a whole. It is worth noting that this perturbation is not localized and contains a remote wave spreading to or from the soliton (thus, probably, being not of much interest, but rather a mere curiousity). However, we want to draw the reader's attention to the way equation (3.6) has been obtained. We shall use the same idea in the study of the $(2+1)$ analogue of the Benjamin-Ono equation.

4 TRANSVERSE INSTABILITY OF THE SOLITONS OF (2+1) BENJAMIN-ONO (SHRIRA) EQUATION

4.1 Solitons of the Shrira Equation

Equation

$$u_t + cu_x + 6uu_x + \hat{G}[u_x] = 0 \qquad (4.1)$$

or its version in the frame fixed on the main flow

$$u_t + 6uu_x + \hat{G}[u_x] = 0$$

clearly has plane solitons

$$u_0 = \frac{2}{3}\frac{S}{1 + (Sx - \Omega t)^2} \qquad (4.2)$$

as one of its solutions - as we mentioned before, on a restricted class of functions, independent of y, the Shrira equation reduces to the Benjamin-Ono equation. In what follows we want to consider a more general class of solutions of (1.7) - solitons propagating at an arbitrary angle α to the main flow

$$u_0 = \frac{2}{3}\frac{S}{1 + (Sx - \Omega t)^2}, \quad \Omega = S^2 \cos\alpha \qquad (4.3)$$

The above dispersion relation contains $\cos\alpha$ as a parameter which can be included either into the expression for the velocity of wave propagation or into the one for the amplitude. This allows us to consider the solitary wave (4.3) either as a wave with a constant amplitude S travelling at a speed $S\cos\alpha$ or as a wave with a constant speed $V = \frac{\Omega}{S}$ having an amplitude $S = \frac{V}{\cos\alpha}$ and a "width" $\Delta = \frac{\cos\alpha}{V}$.

4.2 Transverse perturbations of the Shrira equation

We have mentioned that the Benjamin-Ono solitons (as well as Shrira solitons propagating at a certain angle) are stable against the longitudinal perturbations. However, the situation changes dramatically when we consider the transverse perturbations. In this case, as we are about to show, the solitons are unstable.

We shall find the equation which allows us to analyze instability. We consider the perturbation $\tilde{u}(\xi, \eta, t) = \theta(\xi)\exp[i(\omega t + k_\eta \eta)]$, with $\theta(\xi)$ being a function with compact support, in the coordinate frame, oriented with the soliton

$$\begin{bmatrix} \xi \\ \eta \end{bmatrix} = \begin{bmatrix} \cos\alpha & \sin a \\ -\sin\alpha & \cos\alpha \end{bmatrix} \cdot \begin{bmatrix} x - ct \\ y \end{bmatrix}$$

with c being the (rescaled) velocity of the main flow (at a fixed depth), and linearize (4.1) obtaining an equation for θ (here θ, ξ, η should not be confused with (2.3))

$$i\omega\theta(\xi) = \partial_x[c\theta(\xi) - 6u_0\theta(\xi) - \frac{1}{2\pi}(k_\eta^2 - \partial_\xi^2)\times$$

$$\times \int \frac{1}{\left[(k'_\xi)^2 + k_\eta^2\right]^{1/2}} \exp[ik'_\xi(\xi - \xi')]\theta(\xi')\partial k'_\xi \partial\xi'] \qquad (4.4)$$

$$\partial_x = \cos\alpha \cdot \partial_\xi - \sin\alpha \cdot ik_\eta$$

To cast this equation in a tractable form we perform the transformation of Section 3, $\phi(q) = \int \tilde{\theta}(q')\exp[-\sigma\,|q - q'|]\partial q'$ where $\tilde{\theta}(q)$ is the Fourier transform of $\theta(\xi)$. The new equation reads

$$\phi_{qq} + [-\sigma^2 - U]\phi = 0 \qquad (4.5)$$

$$U = -\frac{4\sigma^2}{1 + \sigma\Big[q^2 + k_\eta^2\Big]^{1/2} - \frac{\Omega}{q - k_\eta \cdot \tan\alpha}}, \quad \Omega = \frac{\sigma\omega}{\cos\alpha}, \quad \sigma = \frac{1}{c}$$

It is very interesting that this equation presents a Sturm-Liouville problem with the boundary conditions $\phi(\pm\infty) = 0$. Potential U is complex in general (if spectral parameter Ω is complex).

Some further analysis shows that there is an interesting connection between the structure of the levels in potential U and the instability of solitons. This potential is real on the long-wave and short wave instability thresholds, when the imaginary part of ω becomes equal to zero, and complex in-between. A good illustration of the dynamics of the levels in such a potential could be presented for zero angles of propagation. In this case the potential consists of an even real part and an odd imaginary (see section 4.4 for more details). *This means that the real part of an eigenfunction of* (4.5) *is strictly even and the imaginary part is strictly odd, or vise versa.* Thus, the perturbation wave number being equal to 0 at *the long-wave threshold*, the odd one-node eigenfunction of (4.5) is either strictly real or strictly imaginary and the energy $E = -\sigma^2$ corresponds to *the first energy level* in the potential. Further, as k increases the wave function becomes complex, but turns even and either imaginary or real at *the short-wave threshold* where the potential is more shallow ($E = -\sigma^2$ is kept fixed) than at the long-wave threshold. This is the wave function of *the ground state* (see Fig.2.). At greater k the potential U has no level with $E = -\sigma^2$, thus rendering the instability impossible.

It should be noted that equation (4.4) was also obtained in [8]. Using the asymptotic representation of the integrand in (4.4) the problem was restated as an eigenvalue problem for small wave numbers and solved via Hirota's method. Thus obtained growth rate for the quasi-periodic non-linear wave is given by $\gamma^2 = c^2 k_y^2 - k^2[(K-k_x)^2 + k_y^2]$ where K is expressed through the non-linearity parameter ϕ, $K \cdot \sigma = \tan\phi$. This shows that the instability region increases with the increasing non-linearity of the wave (decreasing $K \cdot \sigma$).

4.3 Transverse perturbations of Shrira solitons in long-wave approximation. The critical angle

In this section we apply the small parameter expansion method to obtain the growth rate of the "inclined" solitons in the long-wave limit. For this we expand the potential in equation (4.5) for small k (to simplify the notation we put $\sigma = 1$)

$$U = \frac{-4}{1+|q|}\left(1 + \frac{-\frac{k_\eta^2}{2|q|} + \frac{\Omega}{q} + \frac{\Omega k_\eta \tan\alpha}{q^2}}{1+|q|} + \frac{\frac{\Omega^2}{q^2}}{(1+|q|)^2}\right) \qquad (4.6)$$

Equation (4.5) is reduced to the form

$$\hat{L}[\phi] \equiv (\partial_q^2 - 1 + \frac{4}{1+|q|})\phi = \left(\frac{\frac{4k_\eta^2}{2|q|} - \frac{4\Omega}{q} - \frac{4\Omega k_\eta \tan\alpha}{q^2}}{(1+|q|)^2} - \frac{\frac{4\Omega^2}{q^2}}{(1+|q|)^3}\right)\phi \qquad (4.7)$$

Further, we are looking for the complex frequency and the eigenfunction as a series in a small parameter

$$\Omega = \epsilon\Omega_1 + \epsilon^2\Omega_2 + \epsilon^3\Omega_3 ...$$

$$k_\eta = \epsilon k_\eta^1 + \epsilon^2 k_\eta^2 + \epsilon^3 k_\eta^3 ...$$

$$\phi = \phi_0 + \epsilon\phi_1 + \epsilon^2\phi_2...$$

This will allow us to isolate consecutive orders in equation (4.7). Equating terms of different orders we get

$$\hat{L}[\phi_0] = 0 \qquad (4.8a)$$

$$\hat{L}[\phi_1] = -\frac{4\Omega_1\phi_0}{q(1+|q|)^2} \qquad (4.8b)$$

$$\hat{L}[\phi_2] = -\frac{4\Omega_1\phi_1}{q(1+|q|)^2} - \frac{4\Omega_2\phi_0}{q(1+|q|)^2} - \frac{4\Omega_1 k_\eta^1 \tan\alpha\ \phi_0}{q^2(1+|q|)^2} + \\ + \frac{2\left(k_\eta^1\right)^2\phi_0}{|q|\,(1+|q|)^2} - \frac{4\Omega_1^2\phi_0}{q^2(1+|q|)^3} \qquad (4.8c)$$

The first and the second of these equations can be easily solved to get

$$\phi_0 = q\,(1+|q|)\exp\left[-|q|\right]$$

$$\phi_1 = -\Omega_1\left(\exp\left[-|q|\right] + 2q(1+q)\eta(q)\exp\left[-q\right]\right)$$

with $\eta(q)$ being the step function.

We notice that because of equation (4.8a) and the self-adjoint property of $\hat{L}$ the following condition should necessarily hold for all orders of ϕ

$$\int \phi_0\hat{L}[\phi_i]\partial q = 0 \qquad (4.9)$$

Now, this condition for ϕ_1 is satisfied as can be easily checked. The same condition in the next order gives a non-trivial equation

$$\int \phi_0\hat{L}[\phi_2]\partial q = 0 = \frac{\left(k_\eta^1\right)^2}{2} + \Omega_1^2 - 2k_\eta^1\cdot\tan\alpha\cdot\Omega_1 \qquad (4.10)$$

from which we obtain the dispersion relation in the long-wave limit (we drop the ordering subscripts).

$$\Omega = k_\eta \sin\alpha \pm i\cos\alpha \left(\frac{k_\eta^2}{2} - k_\eta^2 \tan^2\alpha\right)^{\frac{1}{2}} \qquad (4.11)$$

Of the special importance is the fact that this dispersion brings about the existence of a critical angle. Two different scenarios for the growth rate are separated by angle $\alpha_c = \arctan\left[\frac{1}{\sqrt{2}}\right]$. The growth rate itself is given by

$$\gamma = \cos\alpha \cdot \frac{k_\eta}{2^{1/2}} \left(1 - 2\tan^2\alpha\right)^{\frac{1}{2}} \qquad (4.12)$$

and for $\alpha > \alpha_{cr}$ it follows the tendency $\frac{\gamma}{k_\eta} \to 0$ as $k_\eta \to 0$. For $\alpha < \alpha_{cr}$, $\frac{\gamma}{k_\eta} \to const.$

It is worth noting that the case of $\alpha = 0$ yeilds $\omega = 0$ and $\gamma = \frac{k_\eta}{\sqrt{2}}$. This result has been previously obtained in [6].

The above analysis shows that in the long-wave approximation the decay rate grows linearly with the perturbation wave number.

4.4 Numerical Analysis of the Instability

The main result of this paper is the dependence of the instability growth rate and the real frequency on the perturbation wave number for several angles of propagation. To this end we procede to analyze equation (4.5) numerically.

To limit the range of the independent variable in (4.5) we used the following substitution

$$x = \frac{2}{\pi}\arctan(q) \qquad (4.10)$$

Taking into account the fact that in the most general case of an arbitrary angle of propagation the potential in (4.5) is complex, substitution (4.10) transforms the Sturm-Liouville equation (4.5) into an equation for a complex eigenfunction $\phi(x)$

$$\frac{4\cos^4(\frac{\pi x}{2})}{\pi^2}\phi'' - \frac{4\cos^4(\frac{\pi x}{2})\tan(\frac{\pi x}{2})}{\pi}\phi' + \Big(-\sigma^2 - U(x)\Big)\phi = 0 \qquad (4.11)$$

$$U(x) = \frac{-4\sigma^2}{1 + \sigma\Big[\tan(\frac{\pi x}{2})^2 + k_\eta^2\Big]^{1/2} - \frac{\Omega}{\tan(\frac{\pi x}{2}) - k_\eta \cdot \tan\alpha}}$$

We discretize this equation using the standard two-point approximation for the first derivative and three-point approximation for the second derivative, obtaining a linear problem for the vector of point-values of the complex eigenfunction. This problem, of the form $A\mathbf{e} = 0$ with zero boundary conditions at $x = 1$ and $x = -1$, has a non-trivial solution iff complex $\det(A)(\omega, \gamma, k) = 0$ with $\omega = \Re[\Omega]$ and $\gamma = \Im[\Omega]$. We solve this equation for each value of k using the standard $2 - D$ globally convergent Newton method with line search and backtracking [12].

To test the viability of the method we try it on the Sturm-Liouville problem with the soliton-like complex potential

$$U(x) = -\omega\ \text{sech}^2\left(\tan\left(\frac{\pi x}{2}\right)\right) - i\gamma\ \text{sech}^2\left(\tan\left(\frac{\pi x}{2}\right)\right)$$

The real part of this potential is the famous attracting KDV-soliton appearing in the direct problem for the KDV equation. It is a well-known fact that the Sturm-Liouville problem with such complex potential and zero-boundary conditions posses eigenvalue $\lambda = -1$ for $\omega = n(n+1)$, $\gamma = 0$. These values of ω and λ correspond to the $(n-1)^{st}$ energy level in the soliton well (see, for ex., [13]).

We ran our root-finding procedure for several discretizations of the interval $(-1, 1)$. Here we include the results of convergence of ω and γ to the required values for two initial approximation: $\omega = 0.5$, $\gamma = 1.0$ and $\omega = 31.0$, $\gamma = 2.0$. We expect the first set of data converge to $\omega = 2.0$, $\gamma = 0.0$ $(n = 1)$ and the second to $\omega = 30.0$, $\gamma = 0.0$ $(n = 5)$. The values of ω, γ (rounded up to 3 significant figures) and the number of iterations in Newton root-finding are summarized in Tables 1 and 2. For this test the convergence criterion on the function value in Newton procedure was kept at $1.0E-14$, the step convergence criterion at $1.0E-16$ and criterion of convergence on a spurious minimum at $1.0E-15$. For all discretizations Newton root-finding was terminated by step converegnce.

As a further demonstration of the method we include the convergence results of our algorithm for various discretizations of the Sturm-Liouville problem with potential (4.11). The results for for angle $\alpha = \frac{\pi}{6}$ and perturbation wave number $k = 1.0$ are given in Table 3 and Fig.3. The first column is the value of the step used in the discretization of the equation, the second and the fourth columns are the obtained values of ω and γ, the third and the fifth columns show the difference of ω and γ values for two consecutive discretizations. All differences are rounded up to 3 significant figures. The convergence is obviously superlinear and probably quadratic as it should be expected for a second-order scheme.

Thus tested algorithm was used to compute the dispersion curves of the perturbed Shrira equation. The obtained dependencies are pictured in Fig.4. These curves do show the expected behavior: solitons propagating along the flow are the most unstable, instability decreases with the increasing angle of propagation eventually disappearing for perpendicular solitons.

It should be noted that the obtained instability growth rate dependence on the transverse perturbation wave number is quite similar to those typical of many well-known classical non-linear wave models such as KdV, KP and NSE. If a soliton described by this model is unstable against the transverse perturbation then, at the long-wave end of the instability range, growth rate increases with increasing wave number, further, for shorter waves the dynamics is stabilized when the wave-length is of the order of characteristic length defined by dispersion.

In contrast to the earlier obtained results [8], there are no multiple zones of instability within the instability range, rather, there exists a single universal zone of instability, and the short wave threshold turns out constant for all angles of soliton inclination.

In an attempt to justify our predictions of Section 4.3 for the long-wave growth rate behavior we used our numerical scheme for small k and for two angles, above and below the predicted critical angle. Results, shown in Fig.5, do confirm the existence of a critical angle, separating two types of behavior. A remark, however, is in order: we were not able to implement the algorithm all the way to $k = 0$. For very small k and Ω the potential becomes very irregular and our numerical scheme produces (spurious) oscilations in the dispersion curves. Despite of this, tendencies of $\frac{\gamma}{k}$ for angles above and below critical are obviously in accord with predictions of Section 4.3.

4.5 Stability of Solitons Propagating Perpendicular to the Main Flow

Let us consider "perpendicular" solitons - solitons moving at angle $\frac{\pi}{2}$ to the main flow. In accordance with two approaches to a solitary wave outlined in Section 4.1, these "perpendicular" waves could be viewed as waves with either amplitude or velocity independent of the angle. The former are the waves with the phase velocity $V = \frac{\Omega}{S} = S\cos\alpha = S\cos\frac{\pi}{2} = 0$

$$u_0 = \frac{2}{3}\frac{S}{1+(S\xi)^2} \qquad (4.12)$$

the latter are the δ-waves with the amplitude $S = \frac{V}{\cos\alpha} \to \infty$ for $\alpha \to \frac{\pi}{2}$, that is

$$u_0 = \frac{2}{3}\pi\delta(\xi - Vt) \qquad (4.13)$$

We limit our consideration to the long-wave case when equation (4.5) could be rewritten as

$$\phi_{qq} + [-1 - U(q,\alpha)]\phi = 0 \qquad (4.14)$$

$$U = -\frac{4}{1+|q|-\nu}, \qquad \nu = \left[\frac{\Omega\cos\alpha}{k_\eta}\right]_{k_\eta \to 0}$$

where we have put for simplicity $\sigma = 1$ which is equivalent to the change $\sigma \cdot q \to q$. Matching relatively self-suggesting solutions of (4.14) and their derivatives for negative and positive values of q we could find two even solutions

$$\phi_0 = (\nu_0 + |q|)\cdot(1 + \nu_0 + |q|)\exp[-|q|], \quad \nu_0 = \frac{1+\sqrt{5}}{2} \qquad (4.15a)$$

$$\phi_2 = (\nu_2 + |q|)\cdot(1 + \nu_2 + |q|)\exp[-|q|], \quad \nu_2 = \frac{1-\sqrt{5}}{2} \qquad (4.15b)$$

and two odd

$$\phi_1 = q\cdot(1 + |q|)\exp[-|q|], \quad \nu_1 = 0 \qquad (4.15c)$$

$$\phi_3 = q\cdot(1 - |q|)\exp[-|q|], \quad \nu_3 = -1 \qquad (4.15d)$$

It can be seen that the spectral parameter ν_0 corresponds to an eigenfunction without zeros, that is an eigenfunction of the ground state (level) of the potential U ; parameter ν_1 corresponds to the one-node function of the first state; parameter ν_2 corresponds to the eigenfunction of the second state with two nodes; and parameter ν_3 - to the eigenfunction of the third level with three nodes. The depth of the potential is different for these parameter values, while the energy of the corresponding state is constant and equal to -1. Of the special importance is the fact that all parameter values are real. This means that for the solitons (4.12)

$$[k_\eta \nu_i]_{k_\eta \to 0} = [\Omega \cos \alpha]_{\alpha \to \frac{\pi}{2}} = \omega \qquad (4.16)$$

the perturbation frequency is real and the four perturbation modes (4.15) are *stable* . This is in line with (4.12) since the instability growth rate should go to zero faster than k_η for angle larger than the critical, and $\frac{\pi}{2}$ is certainly larger than α_{cr}.

If we think of the " perpendicular" solitons as the δ-solitons we get

$$\nu_i \left[\frac{k_\eta}{\cos \alpha} \right]_{k_\eta \to 0, \alpha \to \frac{\pi}{2}} = \omega$$

The δ-solitons are also stable with respect to the transverse perturbations. This perturbation is not stationary in the limiting case of $\left[\frac{k_\eta}{\cos \alpha} \right]_{k_\eta \to 0, \alpha \to \frac{\pi}{2}} \to$ *const*. We want to note, however, that the consideration of solitons with a vary large (in the limit, infinitely large) amplitude within the framework of the model is somewhat awkward. The appearance of the δ-solitons is an artifact of our two-sided approach to incorporating $\cos \alpha$ into the dispersion relation (Section 4.1); thus thinking of the "inclined" solitons as waves with the amplitude independent of the angle and varying velocity should be more natural.

5 CONCLUSION

We have considered stable and unstable dynamics of solitons in boundary and surface layers of shear hydrodynamic flows. Several aforementioned results are worth emphasizing.

First, the value of the short-wave threshold of the longitudinal perturbation of the solitons turned out to be constant and independent of the angle of propagation of the soliton with respect to the main shear flow. We determined this value numerically to be $\frac{k_{th}}{c} = 2.2625 \pm 0.0005$ where c is the velocity of the main flow.

Second, using numerical methods we found the dependence of the instability growth rate and the real frequency on the perturbation wave number for several angles of propagation. Numerical calculations show that the maximum of the growth rate decreases with the growth of the propagation angle and becomes equal zero for $\frac{\pi}{2}$. For a fixed angle both the growth rate and the real frequency monotonously grow with the perturbation wave number to a certain maximum, then monotonously decrease and become equal zero at the short-wave threshold.

Third, solitons propagating at a right angle to the main flow are known to be stable. We have found four stable transverse perturbation modes for such waves.

Lastly, analytic considerations allow us to predict the character of the growth rate dependency on the propagation angle for long waves. We have shown that there should exist a critical angle of propagation in the long-wave limit which serves as a border between two different behaviors of the growth rate: $\frac{\gamma}{k_\eta} \to 0$ for $\alpha > \alpha_{cr}$ and $\frac{\gamma}{k_\eta} \to const$ for $\alpha < \alpha_{cr}$.

6 REFERENCES

References

[1] T. B. Benjamin. *Internal waves of permanent form in fluids of great depth, J. Fluid Mech., 1967, vol. 29, #3, p. 559.*

[2] H. Ono. *Algebraic solitary waves in stratified fluids, J. Phys. Soc. Jap., 1975, vol. 39, #4, p. 1082.*

[3] V. I. Shrira. *On surface waves in the upper quasi-uniform ocean layer. Dokl. Akad. Nauk SSSR, 1989, vol. 308, #3, p. 732.*

[4] R. Hirota. *Lecture Notes in Physics, 1976, vol. 515.*

[5] J. Satsuma and Y. Ishimori. *Periodic wave and rational soliton solutions of the Benjamin-Ono equation, J. Phys. Soc. Jap., 1979, vol. 46, #2, p. 681.*

[6] A. N. Dyachenko and E. A. Kuznetsov. *Instability and self-focusing of solitons in the boundary layer, JETPh Letters, 1994, vol. 59, #2, p. 108.*

[7] L. A. Abramyan, Yu. A. Stepanyants, V. I. Shrira. *Multidimensional solitons in shear flows of the boundary-layer type, Sov. Phys. Dokl., 1992, vol. 37, #12, p. 575.*

[8] D. A. Pelinovsky, Yu. A. Stepanyants. *Self-focusing instability of solitons in shear flows. JETPh, 1994, vol. 78, #6, p. 883.*

[9] Y. Serizawa, T. Wantanabe, M. B. Chaudhry, and K. Nishikawa. J. *A numerical method for eigenvalue problems of integral equations, J. Phys. Soc. Jap., 1983, vol 52, #1, p. 28.*

[10] A. B. Mikhailovskii. *Theory of Plasma Instabilities, New York, 1975.*

[11] V. I. Petviashvili. *Solitary Waves in Plasmas and in the Atmosphere, Philadelphia, 1992.*

[12] W. H. Press et al. *Numerical Recipes in Fortran. The Art of Scientific Computing, Cambridge, 1992.*

[13] G. L. Lamb *Elements of Soliton Theory, New York: Wiley, 1980.*

7 List of figure captions

1. *Fig.1a.* Example of a free surface flow profile. *Fig.1b.* Example of a boundary flow profile.

2. *Fig.2a.* Energy levels at the long-wave instability threshold: the ground state (solid line) and the first "excited" state (dashed line). *Fig.2b.* Energy levels at the short-wave instability threshold: the ground state (solid line).

3. *Fig.3a.* ω as a function of discretization step. $\alpha = \frac{\pi}{6}$, $k = 1.0$. *Fig.3b.* γ as a function of discretization step. $\alpha = \frac{\pi}{6}$, $k = 1.0$.

4. *Fig.4a.* Dependence of the real frequency, ω, on wave number, k, for several angles of propagation (in radians, top to bottom): $\frac{\pi}{4}$, 0.62, 0.60, $\frac{\pi}{6}$, $\frac{\pi}{8}$, $\frac{\pi}{16}$, $\frac{\pi}{24}$. (*Remark* : frequency curve for angle 0 coincides with the horizontal axis). *Fig.4b.* Dependence of the growth rate, γ, on wave number, k, for several angles of propogation (in radians, top to bottom): 0, $\frac{\pi}{24}$, $\frac{\pi}{16}$, $\frac{\pi}{8}$, $\frac{\pi}{6}$, 0.60, 0.62, $\frac{\pi}{4}$.

5. *Fig.5.* Dependence of the growth rate divided by the wave number, Γ, on the wave number, k, for two angles of propagation, above and below critical, $\frac{\pi}{6}$ (upper curve) and $\frac{\pi}{4}$ (lower curve).

8 Tables

number of points	$\omega - n(n+1)$	γ	number of iterations
100	$-8.07\text{E}-04$	$-8.90\text{E}-07$	11
500	$-3.36\text{E}-05$	$-7.50\text{E}-07$	10
1000	$-9.37\text{E}-06$	$-7.51\text{E}-07$	12
2000	$-3.31\text{E}-06$	$-7.46\text{E}-07$	11
3000	$-2.20\text{E}-06$	$-7.51\text{E}-07$	15
4000	$-1.81\text{E}-06$	$-7.54\text{E}-07$	16

Tab.1. Values of ω and γ for initial data $\omega = 0.5$ and $\gamma = 1.0$

number of points	$\omega - n(n+1)$	γ	number of iterations
100	2.76	$-7.63\text{E}-07$	7
500	$-1.21\text{E}-02$	$4.86\text{E}-07$	7
1000	$-3.05\text{E}-03$	$4.72\text{E}-07$	8
2000	$-7.77\text{E}-04$	$4.39\text{E}-07$	7
3000	$-3.56\text{E}-04$	$4.32\text{E}-07$	7
4000	$-2.08\text{E}-04$	$4.30\text{E}-07$	8

Tab.2. Values of ω and γ for initial data $\omega = 31.0$ and $\gamma = 2.0$

h_i	ω_i	$\omega_i - \omega_{i-1}$	γ_i	$\gamma_i - \gamma_{i-1}$
2.0E − 02	0.391165562		0.338741227	
4.0E − 03	0.391145659	−1.99E − 5	0.339520253	7.79E − 4
2.0E − 03	0.391144974	−6.85E − 7	0.339544804	2.45E − 5
1.0E − 03	0.391144802	−1.72E − 7	0.339550943	6.12E − 6
6.6(6)E − 04	0.391144769	−3.3E − 8	0.339552079	1.14E − 6
5.0E − 04	0.391144758	−1.1E − 8	0.339552477	3.98E − 7
4.0E − 04	0.391144753	−5.0E − 9	0.339552661	1.84E − 7
3.51E − 04	0.39114475	−3.0E − 9	0.339552737	7.6E − 8

Tab.3. Convergence of the real frequency and the growth rate for several discretizations of (4.11).

Fig.1a

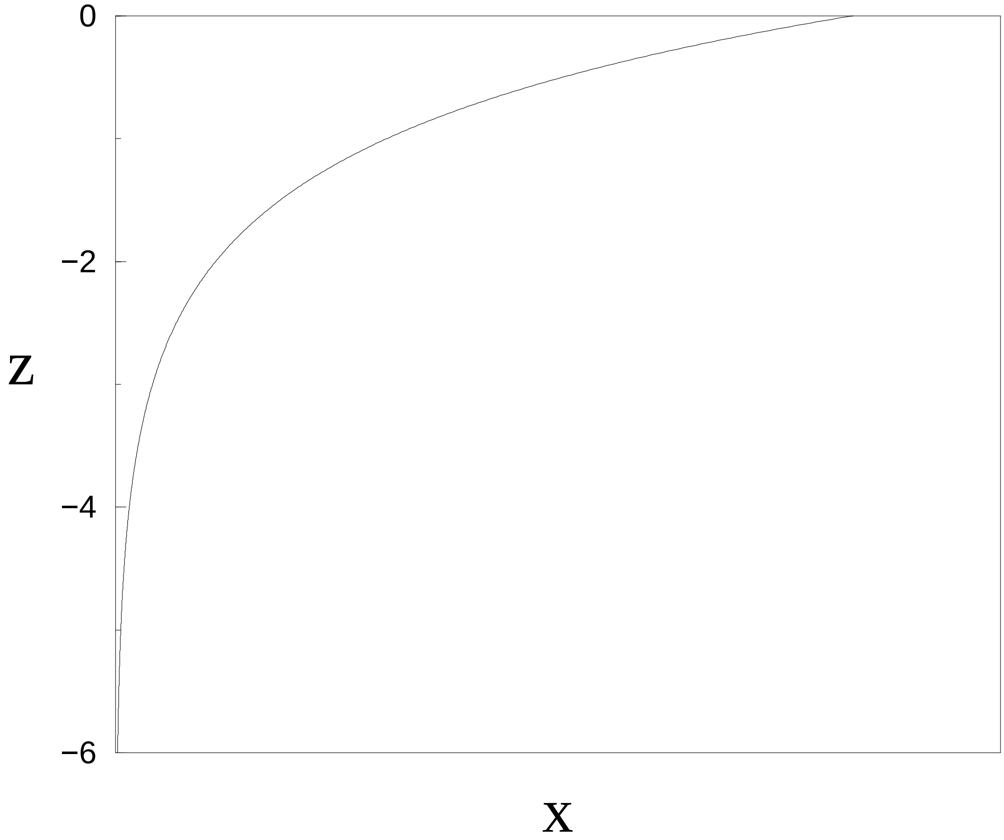

Fig.1b

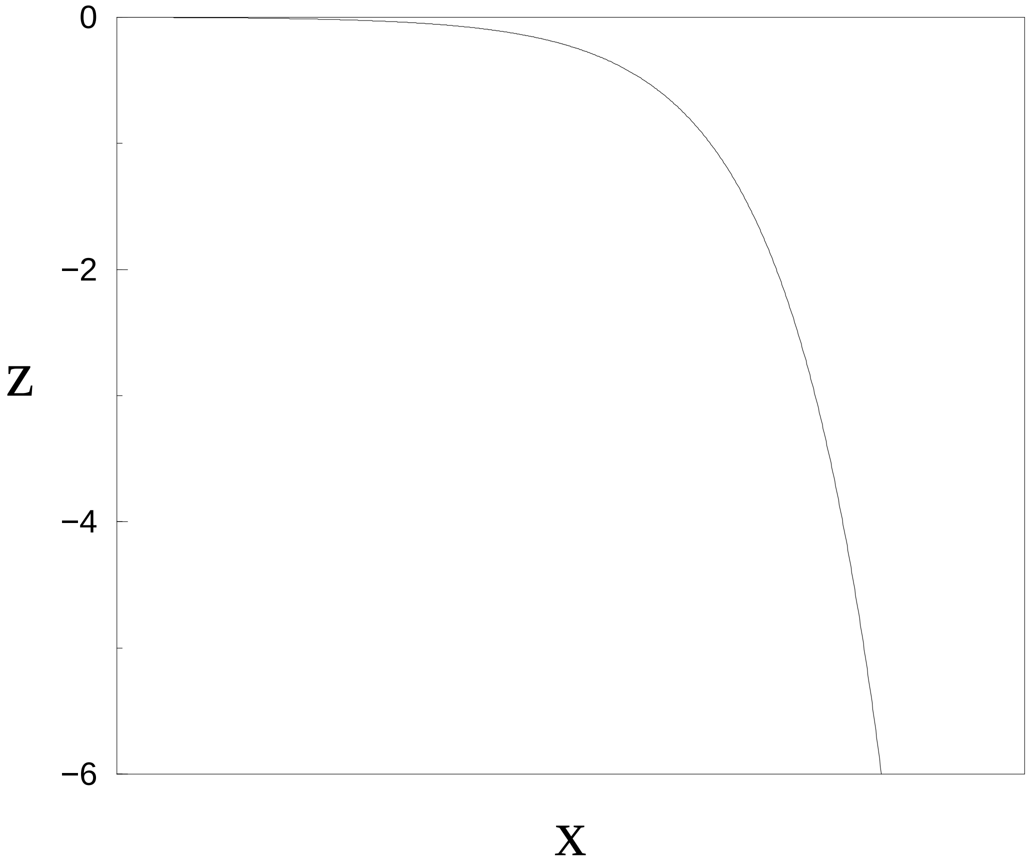

Fig.2a.

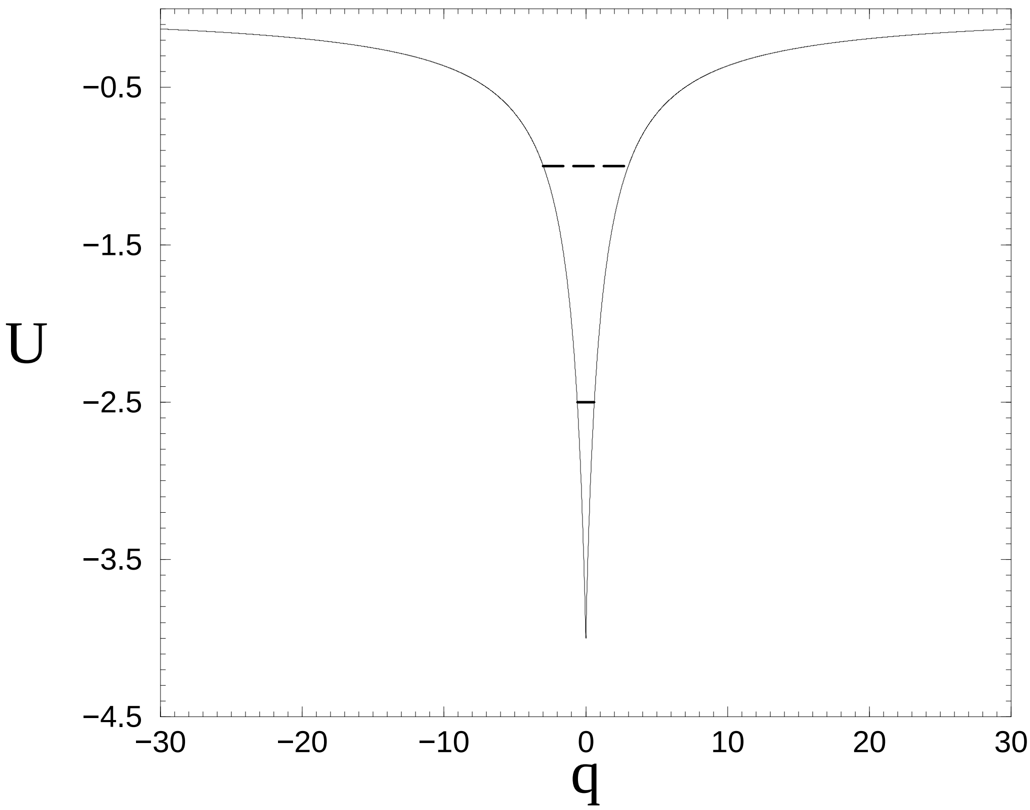

Fig.2b.

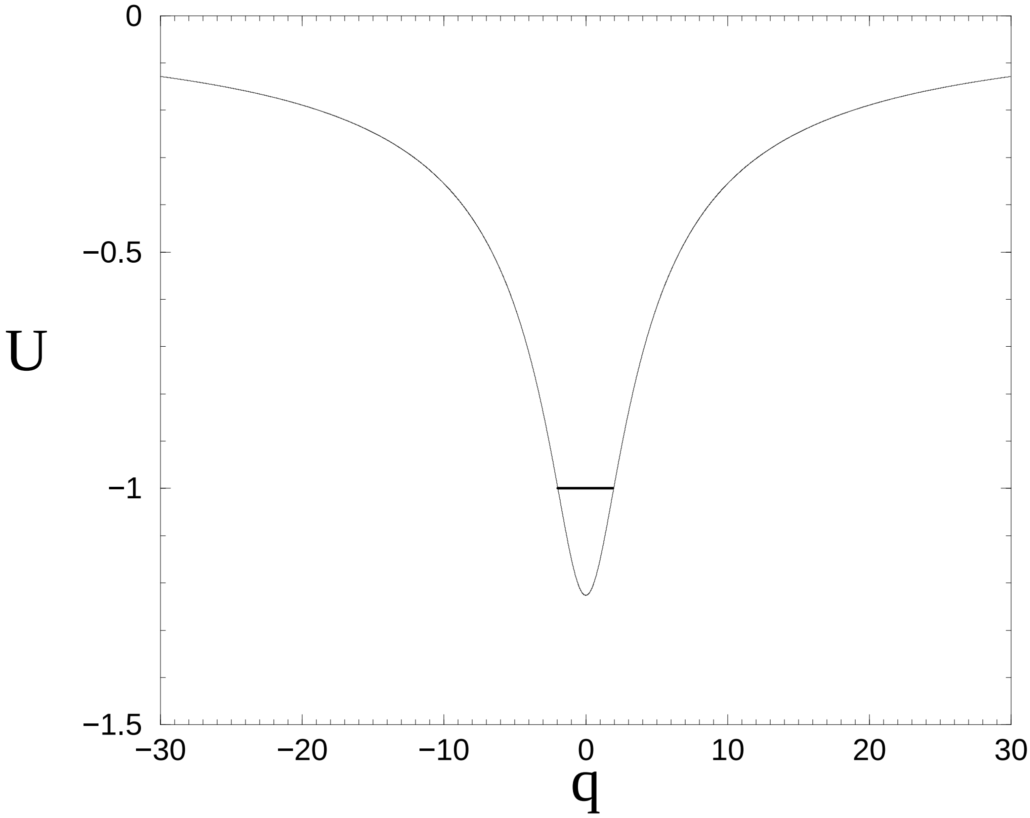

Fig.3a.

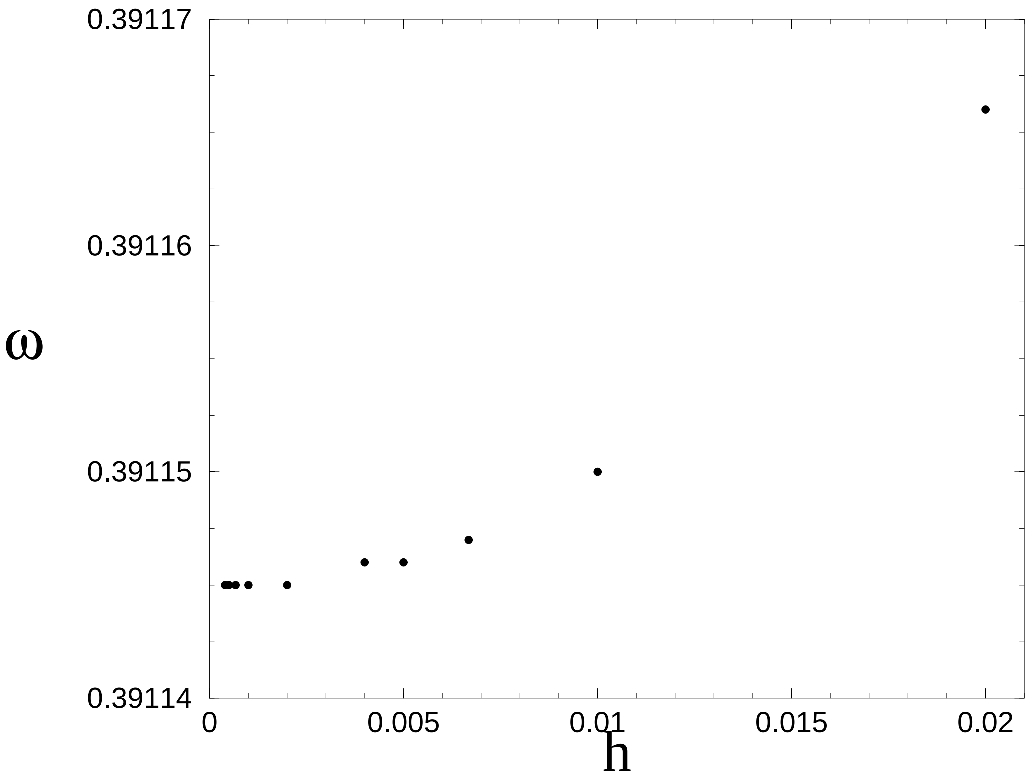

Fig.3b.

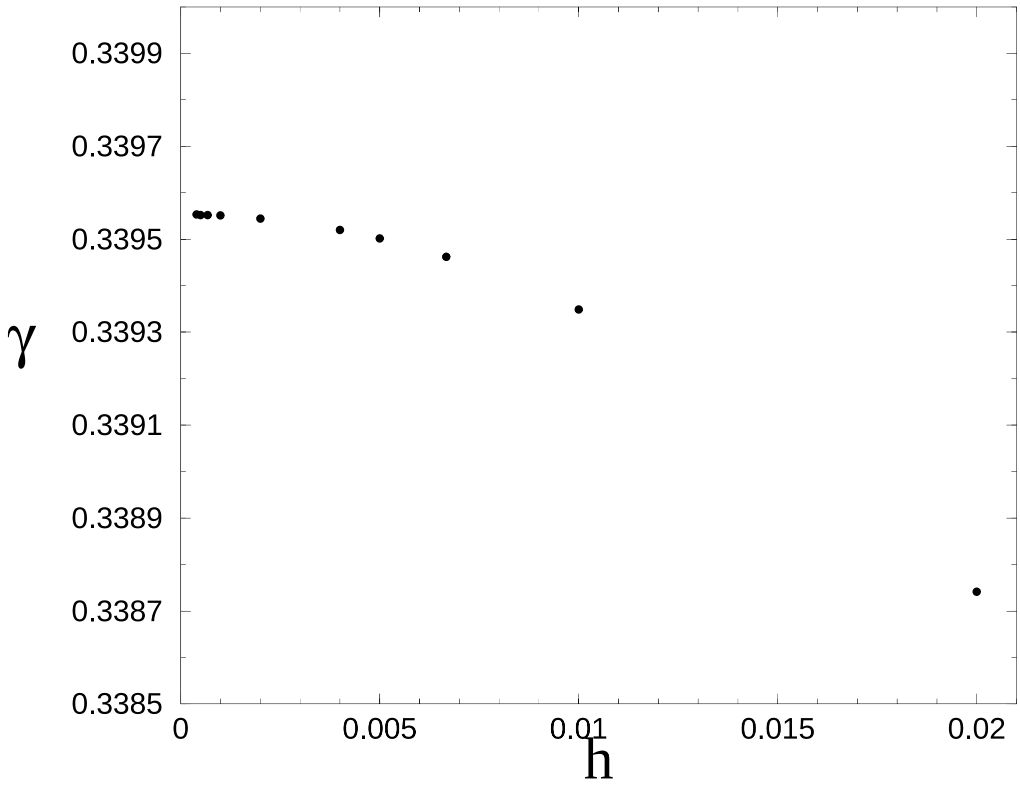

0.3399
0.3397
0.3395
0.3393
0.3391
0.3389
0.3387
0.3385
γ
0
0.005
0.01
0.015
0.02
h

Fig.4a.

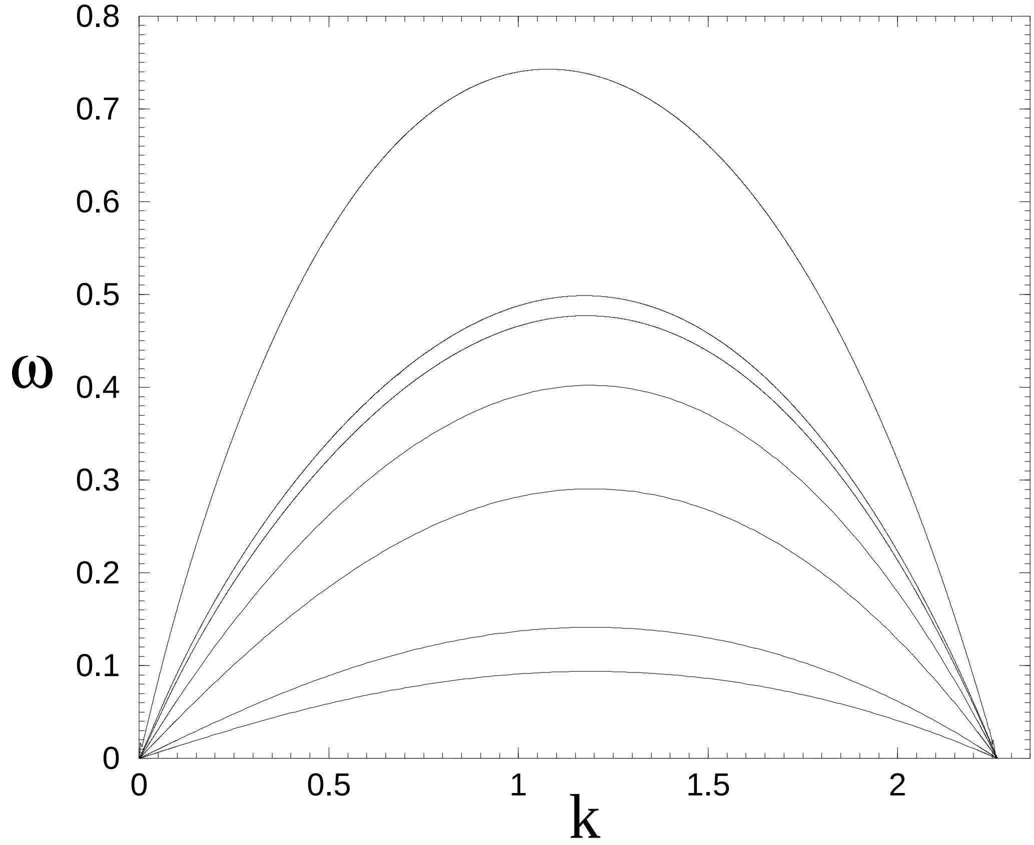

Fig.4b.

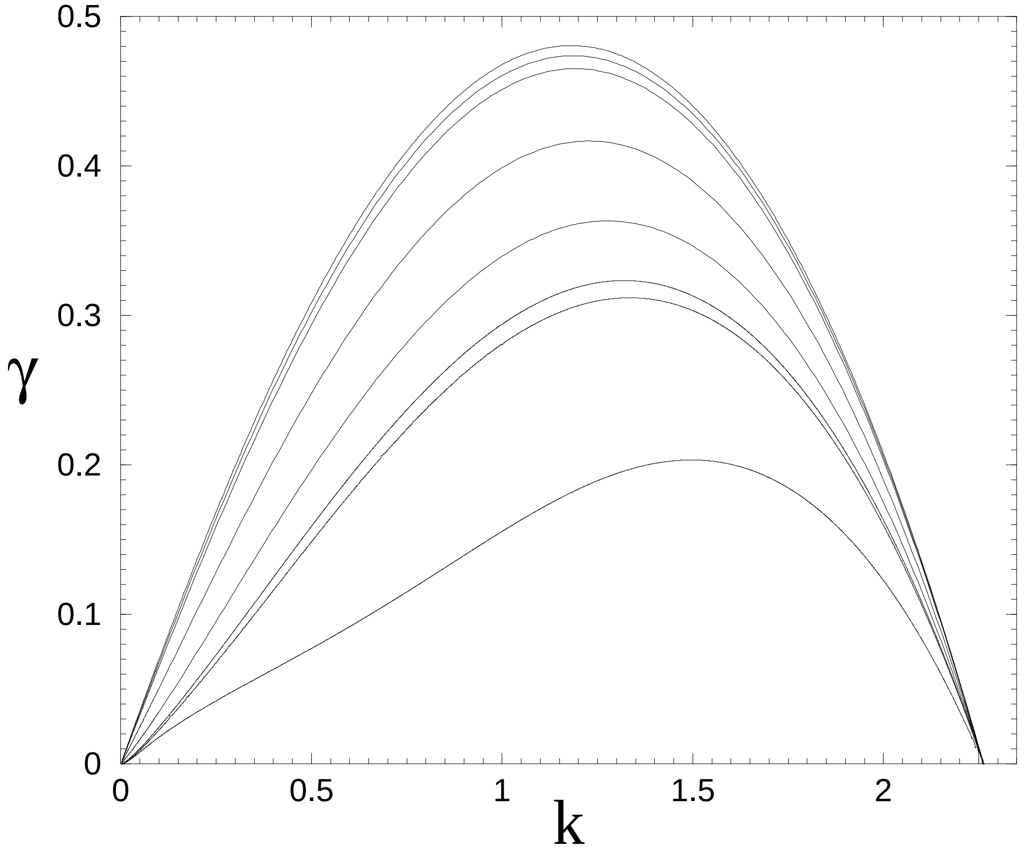

Fig. 5.